Ultrafast photoinduced mechanical strain in epitaxial BiFeO3 thin films

L. Y. Chen, J. C. Yang, C. W. Luo, C. W. Laing, K. H. Wu, J.-Y. Lin, T. M. Uen, J. Y. Juang, Y. H. Chu, and T. Kobayashi

Articles you may be interested in

The conduction mechanism of large on/off ferroelectric diode currents in epitaxial (111) BiFeO3 thin film
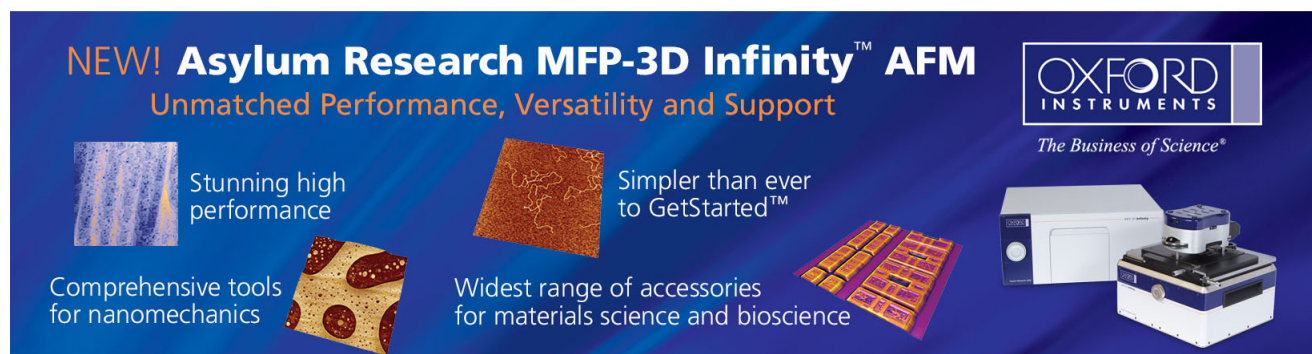J. Appl. Phys. **113**, 184106 (2013); 10.1063/1.4804144

Strain modulated transient photostriction in La and Nb codoped multiferroic BiFeO3 thin films
Appl. Phys. Lett. **101**, 242902 (2012); 10.1063/1.4770309

Structural study in highly compressed BiFeO3 epitaxial thin films on YAlO3
J. Appl. Phys. **112**, 052002 (2012); 10.1063/1.4746036

X-ray nanodiffraction of tilted domains in a poled epitaxial BiFeO3 thin film
Appl. Phys. Lett. **99**, 232903 (2011); 10.1063/1.3665627

Nanoscale domains in strained epitaxial BiFeO 3 thin Films on LaSrAlO 4 substrate
Appl. Phys. Lett. **96**, 252903 (2010); 10.1063/1.3456729

Ultrafast photoinduced mechanical strain in epitaxial BiFeO₃ thin films

L. Y. Chen,[1] J. C. Yang,[2] C. W. Luo,[1,a)] C. W. Laing,[2] K. H. Wu,[1] J.-Y. Lin,[3] T. M. Uen,[1]
J. Y. Juang,[1] Y. H. Chu,[2] and T. Kobayashi[1,4]

[1]*Department of Electrophysics, National Chiao Tung University, Hsinchu 300, Taiwan*
[2]*Department of Materials Science and Engineering, National Chiao Tung University, Hsinchu 300, Taiwan*
[3]*Institute of Physics, National Chiao Tung University, Hsinchu 300, Taiwan*
[4]*Advanced Ultrafast Laser Research Center, and Department of Engineering Science, Faculty of Informatics
and Engineering, University of Electro-Communications, 1-5-1Chofugaoka, Chofu, Tokyo 182-8585, Japan*

We studied ultrafast dynamics and photoinduced mechanical strain of BiFeO₃ thin films by dual-color transient reflectivity measurements ($\Delta R/R$). Anisotropic photostriction in BiFeO₃ is found to be mainly driven by the optical rectification effect. Results of the photostriction at various thicknesses show that the estimated sound velocity along [110] direction of BiFeO₃ is 4.76 km/s. © *2012 American Institute of Physics.* [http://dx.doi.org/10.1063/1.4734512]

Multiferroic materials possess ferroelastic, ferroelectric, and anti/ferromagnetic orders simultaneously[1] and are promising for the applications of next-generation devices with combined functionalities. Among various multiferroic candidates, BiFeO₃ (BFO) stands out because of its strong coupling between structural, ferroelectric, and antiferromagnetic orders at room temperature.[2] Recently, Rovillain *et al.*[3] demonstrated an important paradigm for magnonics through such strong coupling between magnetic and ferroelectric order parameters, i.e., the spin waves in BFO can be directly controlled by an electric-field at room temperature. Moreover, the recent discoveries of photovoltaic effect,[4] photo-induced size change,[5,6] and photo-assisted THz emission[7] in BFO have received considerable attention because these nontrivial light-BFO interactions may open applications in optoelectronics and optomechanics, e.g., heterostructure diode,[8] photovoltaic cells,[9] deformable optical cavities.[10] While these discoveries are tantalizing, understanding the physics behind the photon-BFO interactions, including the dynamics of the photo-induced electronic excitation in BFO as well as its coupling with multiferroic orders, e.g., spin, orbit, and electric dipole, remains elusive and is yet to be studied. Femtosecond pump-probe spectroscopy has been established as a protocol to study the interactions between electrons, phonons, and magnons[11–14] and is therefore employed in this work to gain insight into the excitation dynamics in epitaxial BFO thin films.

In this letter, we have investigated the ultrafast photostriction effect in BFO thin films by dual-color pump-probe measurements. We found the anisotropic photostriction in BFO is mainly driven by the optical rectification effect which demonstrates BFO would be a favorable material for the applications of ultrafast photoelastic, optoelectronic, and optomechanical devices through this non-thermal ultrafast process.

Samples used in this study are epitaxial BFO (110) thin films grown on SrTiO₃ (110) single crystal substrates by pulsed laser deposition. Film thickness was carefully con-

trolled via tuning the deposition time and determined by the x-ray reflectivity technique. Details of the deposition procedure have been reported elsewhere in Ref. 15. The femtosecond spectroscopy measurement was performed using a commercial Ti:sapphire laser (repetition rate: 5.2 MHz, wavelength: 800 nm, pulse duration: 70 fs) and a homemade dual-color pump-probe system with the standard lock-in technique at 260 K. The fluences of the pump beam and the probe beam are 2 and 0.1 μJ/cm², respectively. The pump pulses have corresponding photon energy (3.1 eV) beyond the band gap of BFO (2.67 eV)[16] and hence can generate electronic excitations within 40 nm due to the absorption length at $\lambda = 400$ nm.[17] Excitation dynamics is studied by measuring the photoinduced transient reflectivity changes ($\Delta R/R$) of the probe beam with photon energy of 1.55 eV in the depth of >1 μm due to the large absorption length at $\lambda = 800$ nm in BFO.[17]

Figure 1 shows the photoinduced $\Delta R/R$ in a BFO thin film. Electronic excitations generated by the pump pulses
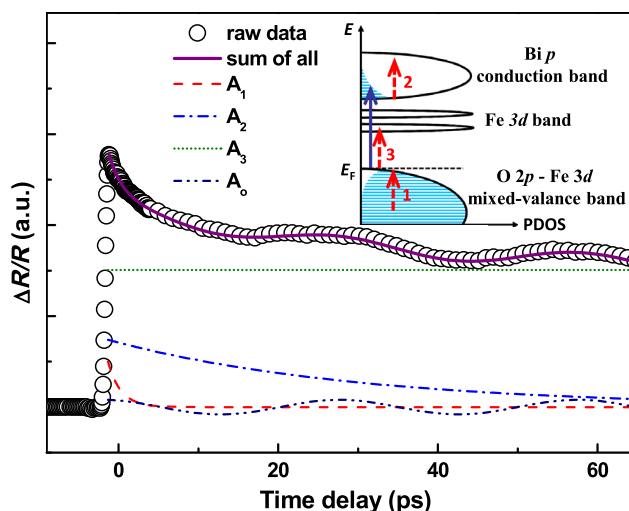

FIG. 1. The typical $\Delta R/R$ curve is fitted by Eq. (1). The inset schematically shows the electronic band structure of BFO (see Refs. 17 and 18) and the pump-probe processes for 3.1-eV-pump (solid arrow) and 1.55-eV-probe (dashed arrows).

a)Author to whom correspondence should be addressed. Electronic mail: cwluo@mail.nctu.edu.tw.

results in a swift rise of $\Delta R/R$ at zero time delay. The observed excitation is triggered by transferring the electrons from $2p$ valence band of O to p conduction band of Bi.[17,18] At zero time delay, number of the excited electrons generated by this non-thermal process is related to the amplitude of $\Delta R/R$. These high-energy electrons accumulated in the p conduction band of Bi release their energy through the emission of longitudinal-optical (LO) phonons within several picoseconds.[19] The LO phonons further decay into acoustic phonons via anharmonic interactions, i.e., transferring energy to the lattice. This relaxation process can be detected using a probe beam, indicated by the process 1 and 2 in the inset of Fig. 1. Special care should be taken because the probe beam could be absorbed by additional electronic transitions in BFO. It has been known that the on-site d-d transition of Fe^{3+} ions (process 3 in the inset of Fig. 1), which should be forbidden due to the total spin of change from $S = 5/2$ to $S = 3/2$,[16] can occur in BFO because the parity selection rule is relaxed through the spin-orbit coupling and the octahedral distortion caused by pump pulses.[16]

The relaxation processes ($t > 0$) represented by $\Delta R/R$ in BFO displays an oscillated feature, which is associated with the strain pulse in oxides,[20] and can be phenomenologically described by

$$\frac{\Delta R}{R} = A_1 e^{-t/\tau_1} + A_2 e^{-t/\tau_2} + A_3 + A_o e^{-t/\tau_o} \cos(2\pi t/T + \phi). \tag{1}$$

The 1st term in the right-hand side of Eq. (1) is the decay of the excited electrons with an initial population number, A_1, and a relaxation time, τ_1 (dashed line in Fig. 1). The 2nd term is the d-d transition of Fe^{3+} ions (process 3) with an absorption probability, A_2, and a corresponding decay time, τ_2 (dash-dotted line in Fig. 1). The 3rd term describes energy loss from the hot spot to the ambient environment within the time scale of microsecond, which is far longer than the period ($\sim$150 ps) of the measurement and hence presented as a constant (dotted line in Fig. 1). The last term is the oscillation component associated with strain pulse propagation: A_o is the amplitude of the oscillation (dash-dot-dotted line in Fig. 1); τ_o is the damping time; T is the period; ϕ is the initial phase of the oscillation.

Figure 2(a) shows $\Delta R/R$ measurements on BFO thin films with various thicknesses (40–360 nm). A discontinuity

is clearly observed in the oscillation feature of $\Delta R/R$ after subtracting the decay background (i.e., the 1st, 2nd, and 3rd terms in Eq. (1)), as shown in the right inset of Fig. 2(a). The amplitude and period of the first oscillation are both larger than those of the second oscillation. This oscillation is caused by the propagation of strain pulses inside the BFO thin film, namely the interference between the probe beams reflected by the thin film surface and the wave front of the propagating strain pulse as illustrated by the cartoon in the inset of Fig. 2(a).[21]

When strain pulses propagate through the BFO/STO interface, both the amplitude and period of the $\Delta R/R$ oscillation decrease. Consequently, the time (denoted by $t_{BFO/STO}$) needed to observe the oscillation discontinuity can be used to extract the speed of the strain pulse, which is equivalent to the sound velocity, in BFO. Results from this experiment show a linear dependence of $t_{BFO/STO}$ on BFO thickness (Fig. 2(b)). The corresponding strain pulse (or sound) velocity, v_{BFO}, along the [110] direction of BFO is estimated to be 4.76 km/s. The strain pulse velocity can be also calculated by using the strain pulse model[21]

$$v_s = \lambda_{probe} \cos \theta / 2 n_{probe} T, \tag{2}$$

where λ_{probe} is the wavelength of probe beam; n_{probe} is the refractive index in probing wavelength; θ is the refractive angle of probe beam in samples; T is the period of oscillation signal in $\Delta R/R$. Using $\lambda_{probe} = 800$ nm, $n_{probe} = 2.8$ (Ref. 22), $\theta = 3.6°$ (estimated from the incident angle (10°) of the probe beam by Snell's law) and $T = 29.2$ ps, the strain pulse velocity, v_s, is calculated to be 4.88 km/s, which is very close to the result, $v_{BFO} = 4.76$ km/s, obtained from our thickness-dependent $t_{BFO/STO}$ measurement. Recently, Smirnova *et al.*[23] also obtained the strain velocity of 4.31 km/s in BFO ceramics at 300 K by using pulse-echo technique at a frequency 10 MHz. A close look at the $\Delta R/R$ signal around zero time delay (shown in the inset of Fig. 2(b)) reveals that the oscillation signal starts within the time scale of ps. This suggests that the time needed to generate strain pulses in BFO is within the time scale of ps. The ultrafast generation of strain pulses in BFO post interesting questions on the mechanisms that drive the ultrafast photostriction in BFO.

To explore the origin and physics behind the ultrafast photostriction in BFO, further studies of the dependence of $\Delta R/R$ on the azimuth angle (ϕ) as well as the laser
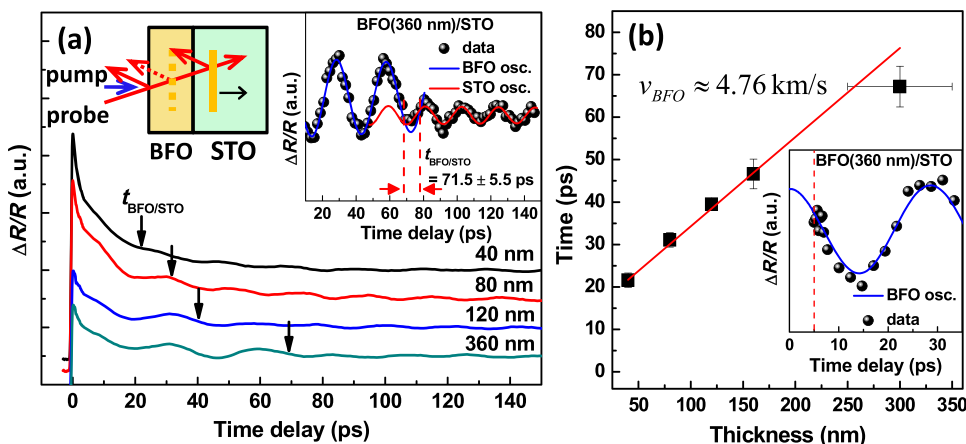

FIG. 2. (a) The $\Delta R/R$ on (110) BFO thin films with various thicknesses. The arrows indicate the BFO/STO interface. Left inset: schematic illustration of the propagation of strain pulse inside BFO and STO substrate. Right inset: the oscillation signal was obtained by subtracted the decay background (the 1st-3rd terms in Eq. (1)) from $\Delta R/R$ of (a). Solid lines are the sinusoidal fitting. (b) The thickness-dependent strain pulse propagating time ($t_{BFO/STO}$) through the interface between BFO and STO. Solid line is the linear fitting curve. Inset shows a part of the right inset in (a) on an enlarged scale.

polarization angle (θ) have been carried out (Fig. 3). The set-up of the $\Delta R/R$ measurements with a variable azimuth angle is illustrated in Fig. 3(a). Results show that $\Delta R/R$ at $t = 0$ s does not change with the azimuth angle of the substrate (Fig. 3(b)), indicating that the photo-induced excitation is isotropic in BFO thin films. Namely, the total number of photo-excited electron-hole pairs keeps constant with varying the azimuth angle of substrate. According to the scenarios commonly used as the explanations for strain pulse generation in polar materials, including (i) electron-hole deformation potential mechanism induced by pump pulses, (ii) electrostrictive effect created by separating of the electron-hole pairs, and (iii) the thermal expansion of lattice due to hot carriers transfer energy to lattice,[24] the strain pulses generated from photostriction in BFO should be isotropic when the pumping fluence used is the same so that the photo-excited electron-hole pairs are kept constant in number. However, our results show that the oscillation amplitude of $\Delta R/R$ is not isotropic but strongly depends on ϕ, as manifested in the inset of Fig. 3(b) which can be further separated into the isotropic part and anisotropic part with nodes. This finding indicates that the aforementioned models still work for the isotropic strain pulse generation in BFO but are insufficient to explain the observed anisotropic $\Delta R/R$ oscillation in our experiments, and therefore alternative explanations are needed.

Further insight into the anisotropic photostriction in BFO is provided by the study of the correlation between the oscillation amplitude of $\Delta R/R$ and the ferroelectric polarization of the BFO thin films. In order to avoid the birefringence effect in the (110) BFO thin film, which also contributes ϕ-dependent oscillation signals, the polarization of the probe beam and the angle of the sample were both fixed. Only the polarization of the pump beam is rotated (Fig. 3(c)). The oscillation amplitude was found to be maximum when the polarization of the pump beam is rotated 90° and 270° against the in-plane component of the ferroelectric polarization (P), while the minimum of the oscillation amplitude is observed at rotation angles of 0° and 180°, as shown in Fig. 3(d). The observed two-fold symmetry of photostriction in BFO with a minimum-to-maximum ratio of 21% is consistent with the results obtained by Kundys *et al.* from bulk BFO crystals.[5] The same symmetry and minimum-to-maximum ratio (~19%) are also observed in the envelope of second harmonic generation (SHG) pattern[25] in (110) BFO thin films, strongly indicating the anisotropic photostriction effect and the SHG in (110) BFO thin films share a common physical origin.

In nonlinear materials, the second-order polarization (P) can be described by

$$P^{(2)}(t) = \varepsilon_0 \chi^{(2)} E(t) E^*(t) = P_0^{(2)}(t) + P_{2\omega}^{(2)}(t), \qquad (3)$$

where $\chi^{(2)}$ is the nonlinear susceptibility; $E(t)$ and $E^*(t)$ are the optical electric fields. The 1st term at the right side of Eq. (3) is the optically induced polarization to acquire a dc term, i.e., the so-called optical rectification effect,[26] and the 2nd term is associated with the SHG. Here, we argue that the optical rectification is responsible for the ultrafast anisotropic photostriction in BFO based on that the optical rectification and the SHG in nonlinear materials are derived from a common nonlinear susceptibility ($\chi^{(2)}$), which is a function of ferroelectric polarization. While an intensity-modulated laser pulse would produce a dc electric field inside materials within the pulse duration of femtosecond time scale, an ultrafast strain stress in BFO can be generated via electrostrictive effect which is anisotropic due to the specific direction of ferroelectric polarization (P) as shown in Figs. 3(a) and 3(c). Moreover, the nodal feature in the symmetry of optical rectification like SHG pattern in Fig. 3(d) is smeared by the isotropic excitation of electron-hole pairs, which is revealed in the indifferentiable $\Delta R/R$ at $t = 0$ s for various azimuth angles in Fig. 3(b), to cause the nodeless photostriction pattern in Fig. 3(d). Our finding of the optical rectification-driven ultrafast anisotropic photostriction with the time scale of optical coherence (pulse duration) in BFO is far shorter than
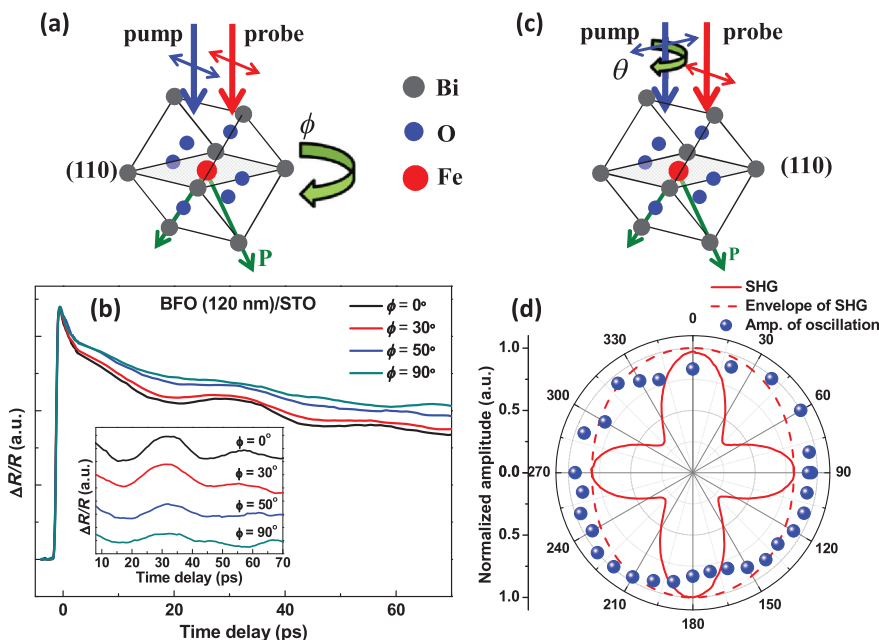

FIG. 3. (a) The experimental configuration for (b). (b) The measurements of the azimuth angle (ϕ) dependence of $\Delta R/R$ in (110) BFO thin films. Inset: the oscillation signal was obtained by subtracted the decay background (the 1st-3rd terms in Eq. (1)) from $\Delta R/R$ of (b). (c) The experimental configuration for (d). (d) The amplitude of oscillation signal of BFO (in the inset of Fig. 2(b)) in $\Delta R/R$ and the intensity of the second harmonic generation as a function of the polarization angle (θ) of pump beam. 0°: the polarizations of both pump and probe beams are parallel to the in-plane component of electric polarization (P) in a (110) BFO thin film. The red-solid line is the θ-dependent SHG intensity. The red-dashed line is the envelope of SHG intensity, and its symmetry is similar with the anisotropic photostriction (solid dots).

that reported by Kundys *et al.* (<0.1 s, obtained under the limited time resolution of measuring systems[5]).

In summary, we have studied the ultrafast dynamics and photostriction in (110) BFO/STO thin films by dual-color femtosecond spectroscopy. By varying the thin-film thickness, which effectively changes strain pulse propagation time, the sound velocity along [110] direction of BFO thin films is obtained and found to be 4.76 km/s. The ultrafast anisotropic photostriction in BFO is found to be mainly derived from the optical rectification effect. Our results provide basic understanding on how photon interacts with multiferroicity in BFO and opens pathways to design ultrafast device with multifunctionality.

[1]N. A. Hill, J. Phys. Chem. B **104**, 6694(2000).

[2]T. Zhao, A. Scholl, F. ZavaLiche, K. Lee, M. Barry, A. Doran, M. P. Cruz, Y. H. Chu, C. Ederer, N. A. Spaldin, R. R. Das, D. M. Kim, S. H. Baek, C. B. Eom, and R. Ramesh, Nat. Mater. **5**, 823 (2006).

[3]P. Rovillain, R. de Sousa, Y. Gallais, A. Sacuto, M. A. Masson, D. Colson, A. Forget, M. Bibes, A. Barthlmy, and M. Cazayous, Nat. Mater. **9**, 975 (2010).

[4]T. Choi, S. Lee, Y. J. Choi, V. Kiryukhin, and S.-W. Cheong, Science **324**, 63 (2009).

[5]B. Kundys, M. Viret, D. Colson, and D. O. Kundy, Nat. Mater. **9**, 803 (2010).

[6]B. Kundys, M. Viret, C. Meny, V. Da Costa, D. Colson, and B. Doudin, Phys. Rev. B **85**, 092301 (2012).

[7]D. S. Rana, I. Kawayama, K. Mavani, K. Takahashi, H. Murakami, and M. Tonouchi, Adv. Mater. **21**, 2881 (2009).

[8]S. R. Basu, L. W. Martin, Y. H. Chu, M. Gajek, R. Ramesh, R. C. Rai, X. Xu, and J. L. Musfeldt, Appl. Phys. Lett. **92**, 091905 (2008).

[9]S. Y. Yang, L. W. Martin, S. J. Byrnes, T. E. Conry, S. R. Basu, D. Paran, L. Reichertz, J. Ihlefeld, C. Adamo, A. Melville, Y.-H. Chu, C.-H. Yang, J. L. Musfeldt, D. G. Schlom, J. W. Ager III, and R. Ramesh, Appl. Phys. Lett. **95**, 062909 (2009).

[10]I. Favero and K. Karrai, Nat. Photonics **3**, 201 (2009).

[11]C. v. K. Schmising, M. Bargheer, M. Kiel, N. Zhavoronkov, M. Woerner, T. Elsaesser, I. Vrejoiu, D. Hesse, and M. Alexe, Phys. Rev. Lett. **98**, 257601 (2007).

[12]D. Talbayev, S. A. Trugman, A. V. Balatsky, T. Kimura, A. J. Taylor, and R. D. Averitt, Phys. Rev. Lett. **101**, 097603 (2008).

[13]C. W. Luo, I. H. Wu, P. C. Cheng, J.-Y. Lin, K. H. Wu, T. M. Uen, J. Y. Juang, T. Kobayashi, D. A. Chareev, O. S. Volkova, and A. N. Vasiliev, Phys. Rev. Lett. **108**, 257006 (2012).

[14]H. C. Shih, T. H. Lin, C. W. Luo, J.-Y. Lin, T. M. Uen, J. Y. Juang, K. H. Wu, J. M. Lee, J. M. Chen, and T. Kobayashi, Phys. Rev. B **80**, 024427 (2009).

[15]Y.-H. Chu, M. P. Cruz, C.-H. Yang, L. W. Martin, P.-L. Yang, J.-X. Zhang, K. Lee, P. Yu, L.-Q. Chen, and R. Ramesh, Adv. Mater. **19**, 2662 (2007).

[16]X. S. Xu, T. V. Brinzari, S. Lee, Y. H. Chu, L. W. Martin, A. Kumar, S. McGill, R. C. Rai, R. Ramesh, V. Gopalan, S. W. Cheong, and J. L. Musfeldt, Phys. Rev. B **79**, 134425 (2009).

[17]M. O. Ramirez, A. Kumar, S. A. Denev, N. J. Podraza, X. S. Xu, R. C. Rai, Y. H. Chu, J. Seidel, L. W. Martin, S.-Y. Yang, E. Saiz, J. F. Ihlefeld, S. Lee, J. Klug, S. W. Cheong, M. J. Bedzyk, O. Auciello, D. G. Schlom, R. Ramesh, J. Orenstein, J. L. Musfeldt, and V. Gopalan, Phys. Rev. B **79**, 224106 (2009).

[18]H. Wang, Y. Zheng, M.-Q. Cai, H. Huang, and H. L. W. Chan, Solid State Commun. **149**, 641 (2009).

[19]F. S. Krasniqi, S. L. Johnson, P. Beaud, M. Kaiser, D. Grolimund, and G. Ingold, Phys. Rev. B **78**, 174302 (2008).

[20]H. C. Shih, L. Y. Chen, C. W. Luo, K. H. Wu, J.-Y. Lin, J. Y. Juang, T. M. Uen, J. M. Lee, J. M. Chen, and T. Kobayashi, New J. Phys. **13**, 053003 (2011).

[21]C. Thomsen, H. T. Grahn, H. J. Maris, and J. Tauc, Phys. Rev. B **34**, 4129 (1986).

[22]A. Kumar, R. C. Rai, N. J. Podraza, S. Denev, M. Ramirez, Y.-H. Chu, L. W. Martin, J. Ihlefeld, T. Heeg, J. Schubert, D. G. Schlom, J. Orenstein, R. Ramesh, R. W. Collins, J. L. Musfeldt, and V. Gopalan, Appl. Phys. Lett. **92**, 121915 (2008).

[23]E. P. Smirnova, A. Sotnikov, S. Ktitorov, N. Zaitseva, H. Schmidt, and M. Weihnacht, Eur. Phys. J. B **83**, 39 (2011).

[24]P. Babilotte, P. Ruello, T. Pezeril, G. Vaudel, D. Mounier, J.-M. Breteau, and V. Gusev, J. Appl. Phys. **109**, 064909 (2011).

[25]The envelope of SHG intensity in Fig. 3(d) with dashed line is plotted by connecting the peaks of the four-fold symmetry pattern in SHG intensity (solid line in Fig. 3(d)) which was also observed in $BiMnO_3$ thin films (Ref. 27).

[26]P. N. Butcher and D. Cotter, *The Elements of Nonlinear Optics, Cambridge Studies in Modern Optics* (Cambridge University Press, Cambridge 1990).

[27]A. Sharan, J. Lettieri, Y. Jia, W. Tian, X. Pan, D. G. Schlom, and V. Gopalan, Phys. Rev. B **69**, 214109 (2004).